

The Regional Thermal Regime in Dixie Valley, Nevada, USA

Mahesh Thakur¹, David D. Blackwell¹, and Kamil Erkan²

¹Huffington Dept. of Earth Sciences, Southern Methodist University, Dallas, Texas, USA

²Department of Civil Engineering, Marmara University, Goztepe, Istanbul, Turkey

Keywords

Dixie Valley EGS project study, heat refraction, 3D subsurface temperatures, pseudogravity, Humboldt lopolith, basement map

ABSTRACT

A three dimensional model for the regional thermal regime of the Dixie Valley /Stillwater Range has been developed as part of the Dixie Valley EGS project. The model is based on a 3D basement map and the assumption of conductive heat transfer. Major variations in heat flow and temperature are due to (1) elevation differences of ~1400 m that cause topographic effects on the subsurface temperatures and (2) the geometry of the ~2 km thick valley fill that causes refraction of heat due to the thermal conductivity difference of approximately a factor of 100% between valley fill and basement/range rock types. A 3D inversion of gravity data is used to obtain a depth map of valley fill sediments. A pseudogravity transformation of magnetic data is used to model the possible effects of the Humboldt mafic igneous complex in the central and northern part of the Dixie Valley. The temperature distribution due to the refraction of heat flow is quantified as a function of the valley fill geometry. Both refraction and topographic effects tend to enhance geothermal gradient in Dixie Valley. Refraction due to the thermal conductivity contrast and shape of the valley fill sediments causes heat flow variation of about 30% of the $90 \pm 30 \text{ mWm}^{-2}$ average regional heat flow. Moderately: high heat flow anomalies along the valley/range contact can be due to refraction of heat flow and may not be caused by geothermal system.

Introduction

The Dixie Valley geothermal district (DVGD) is an active regional scale geothermal system with measured subsurface temperatures of up to 285 °C at a relatively shallow depth of ~ 3 km (Blackwell et al., 2007). The system is non-magmatic in origin based on helium isotope ratios in the geothermal fluids (Kennedy

et al., 2000). Thus the geothermal system is related to deep fluid circulation in an area of high regional heat flow. The extensive exploration activity in the area has resulted in a large data set of geological and geophysical results (Blackwell et al., 2007) that allow a unique characterization of the regional thermal regime in a Basin and Range setting as a help to understand the origin and characteristics of the geothermal occurrences there. DVGD is defined as several systems associated with normal fault zones bounding the Stillwater Range, Dixie Valley, and the Clan Alpine Range. It extends from the Dixie Valley Producing Field (DVPF) on the north to the Dixie Meadows Hot Spring area (DM) on the south (Figure1). Most Basin and Range geothermal systems are fault-controlled, but the detailed structure of the systems is still debated (Wright, 1991). The meteoric water which recharges in the ranges is heated during deep circulation in an area of high heat flow and highly fractured upper crust and ascends along the range bounding fault system (McKenna and Blackwell, 2004; Blackwell et al., 2000; 2007).

Faults that cut sediments in the valley floor adjacent to the main topographic displacement include the piedmont faults (Bell and Katzner, 1987), they are resurfaced so quickly by alluvial and eolian processes that evidence of surface rupture along these faults are quickly buried. Large gravity gradients on the west side to the valley define large structural offset between the basement and valley fill that is 1 km to 2 km basinward of the range/valley contact (Blackwell et al., 1999) and show that along much of the steep east side of the Stillwater Range, piedmont faults in the valley accommodate most of the displacement between the range and the valley bottom.

The objective of this paper is to model the three dimensional steady state subsurface temperature of the Dixie Valley EGS study area (Iovanitti et al., 2011) due to conduction only. The EGS study area is defined by a 50 km x 50 km square (Fig.1) 5 km deep with respect to the valley floor. The study area boundary coordinates in UTM WGS84 as easting and northings are (401500, 4446000), (451500, 4446000), (451500, 4396000), (401500, 4396000). Existing and new thermal data are assembled and analyzed from Dixie Valley to generate and develop a 3-D temperature model and improve the resolution of crustal thermal structure and rock

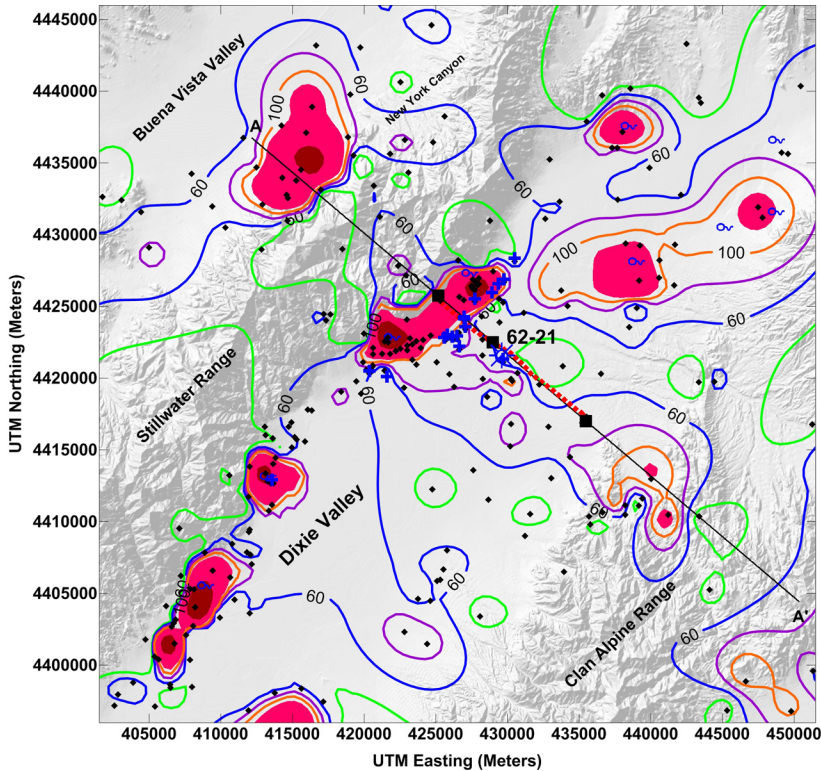


Figure 1. Thermal gradient and well locations of Dixie Valley project area. Contours intervals are 20 °C /km. The contours in pink color represent thermal gradient from 150- 300 °C/Km. Red fill represents thermal gradients more than 300 °C/km – 500 °C/km. Springs in Dixie Valley are shown in blue color. The black squares represent synthetic well locations identified in Figure 7c.

type estimates in the Dixie Valley for development of exploration concepts for EGS geothermal resources using a wide range of geological, geochemical and geophysical data (Iovanitti et al., 2011).

Data: Regional Heat Flow of Dixie Valley

The shallow temperature gradient map of the study area based on 503 thermal gradient wells (less than 500 m deep, Figure 1). Shallow thermal gradient locations in the public domain are shown as black diamonds. Thermal gradient for Dixie Valley study area is contoured using contour interval of 20°C Km⁻¹, contours with geothermal gradient between 150-300°C Km⁻¹ are filled with pink and high geothermal gradients between 300-500°C Km⁻¹ are shown with the dark red fill (Figure 1). The high geothermal gradient anomalies are mainly located along range-valley contacts along the western edge of Dixie Valley (Stillwater Range), and along antithetic faults on the eastern side of Dixie Valley.

Heat flow values for ranges and valleys were averaged separately because of their difference in the topography and the lithology. For calculating the background heat flow within the Dixie Valley, wells that were in the Dixie Valley as were separated from the wells outside of the valley. The task of calculating the background heat flow also required removing all the wells affected by geothermal water circulation; as a result of

this condition wells in the vicinity of anomalies shown were not included in the analysis. For example, most of the wells in the Senator Fumaroles and DVPP were excluded. Using the remaining data, 78 well site locations were used in calculating, the background heat flow.

A frequency distribution of the thermal gradient data used in this analysis area shown in (Figure 2). Most of the data lie between 48-60 °CKm⁻¹. A Gaussian curve fit to the distribution showed a peak at 63 °CKm⁻¹. Parts of the high gradients in the distribution are probably due to the convective transfer of heat and there is no straightforward way to differentiate the convective part from the conductive part. Allowing for some high bias, a gradient of 55 °C Km⁻¹ was chosen to be the best value to represent the purely conductive heat flow in the valley. Measurement of thermal conductivity of various alluvium samples at shallow depth (<200 m) yields

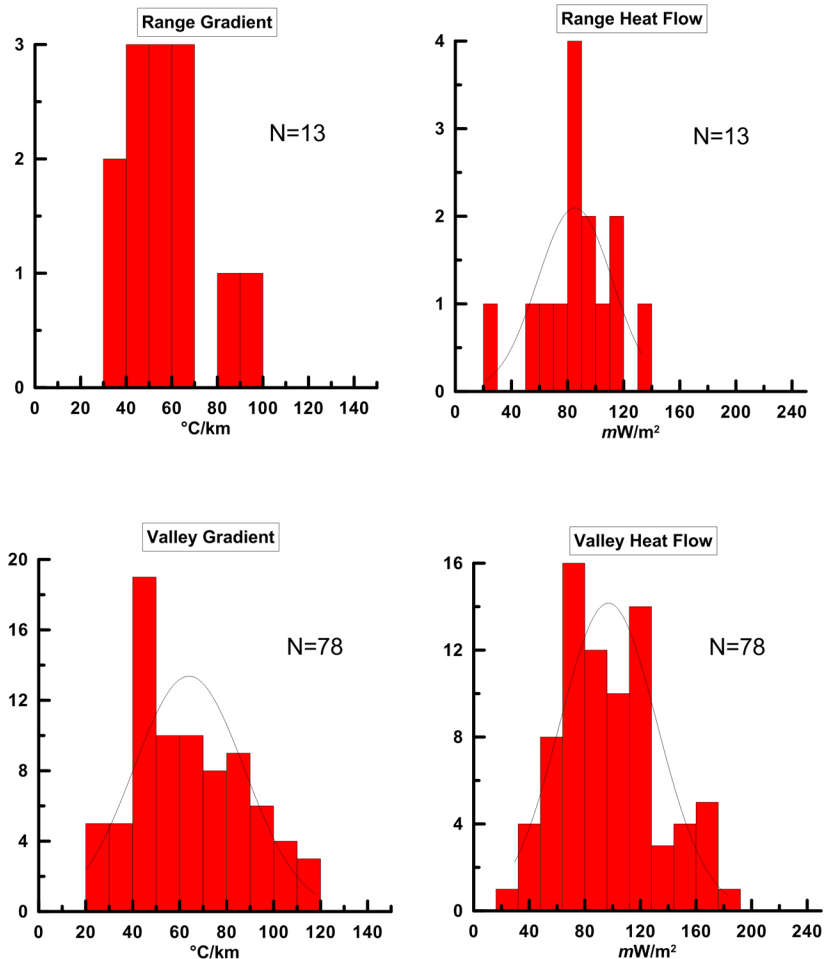


Figure 2. Thermal gradients and heat flow distribution in the Dixie Valley EGS study area.

thermal conductivity values from $1.41\text{--}1.5\text{ Wm}^{-1}\text{K}^{-1}$ (Blackwell et al., 1994). The average thermal conductivity for the shallow part of the valley fill does not vary much and is $1.41\text{--}1.5\text{ Wm}^{-1}\text{K}^{-1}$. Using these values, the background heat flow in the valley is determined to be $81 \pm 3\text{ mWm}^{-2}$.

In analysis of range heat flow, the only 14 wells are available. Thus the range average is poorly determined. Wells that were close to range bounding faults were eliminated from the list because, in these wells, heat flow might be affected from the circulation of geothermal water along the faults and secondly, wells that are close to the edges have significant terrain effects. Since the geology is variable in ranges and there were no samples available, wells were located on a geological map and generic thermal conductivity values were assigned based on lithology. The average value for volcanic rocks was assumed to be $1.4\text{ Wm}^{-1}\text{K}^{-1}$ and the value for intrusive and meta-sedimentary rocks was assumed to be $2.5\text{ Wm}^{-1}\text{K}^{-1}$.

The distribution of heat flow in the ranges as a result of above analysis is shown in Figure 2. The heat flow values are quite dispersed and do not clearly define an average value. The most prominent factors in this data inconsistency are the distortion of regional heat flow due to terrain effects, the small number of available data points, and the lack of thermal conductivity data. Since most of the wells were drilled in small valleys within ranges and the wells are shallow, the apparent heat flow might be higher than the background heat flow in these wells. Looking at distribution, highest frequency is observed around $80\text{--}90\text{ mWm}^{-2}$, which can be considered as the average heat flow in ranges. The wells in the range will be further studied for topographic effects and topographic correction will be applied in order to access the range heat flow. Two large-scale effects play role in the average value of the ranges: First, the terrain effects, which require detailed study of each well to make a viable correction. Second, the refraction effect due to the thermal conductivity contrast between valleys and ranges.

Refraction of heat affects both ranges and valleys. Since valleys are filled with low conductivity materials and ranges are filled with high conductivity material, higher than average heat flow is found in ranges and less than average heat flow is found in valleys (Blackwell, 1983). The regional heat flow in the vicinity of Dixie Valley is 82 mWm^{-2} , which is close to the average heat flow of the Basin and Range region of $85\text{--}90\text{ mWm}^{-2}$ (Lachenbruch and Sass, 1977; Blackwell et al., 1991).

Magnetic Data

The bedrock geology of the Dixie Valley/Stillwater Range area is very complex and the various units have large differences in physical properties that need to be taken into account in preparing synthetic temperature models from non-thermal geophysical data. For example there are large masses of dense, high velocity magnetic mafic rock present in the area, a lithology not typically found in the upper crust. These bodies will affect the interpretation of all the geophysical data. The next sections of the report briefly address the quantification of this problem in a general way. It is discussed in more generally in Blackwell et al. (1997).

High resolution aeromagnetic surveys were flown over part of Dixie Valley (Grauch, 2002). These data reveal subtle, northeast-

trending linear to sinuous features superposed on large amplitude anomalies produced by magnetic bedrock (Grauch, 2002). Unfortunately the high resolution data do not cover the whole study area (see Fig.1, in Grauch, 2002). We downloaded regional magnetic data for all of Nevada from the USGS website (Kucks et al., 2006). The USGS magnetic data for Nevada are girded at a spacing of $1.5\text{--}3\text{ km}$ and depict the magnetic field measured or calculated at 305 m above ground. The Kucks et al. (2006) magnetic data for the study area varies from -400 nT to 1300 nT .

Gravity Data

Four gravity surveys cover the area around and in between Stillwater and Alpine Range. Regional gravity data are available on CD-ROM published by NOAA (Hittelman et al., 1994). These

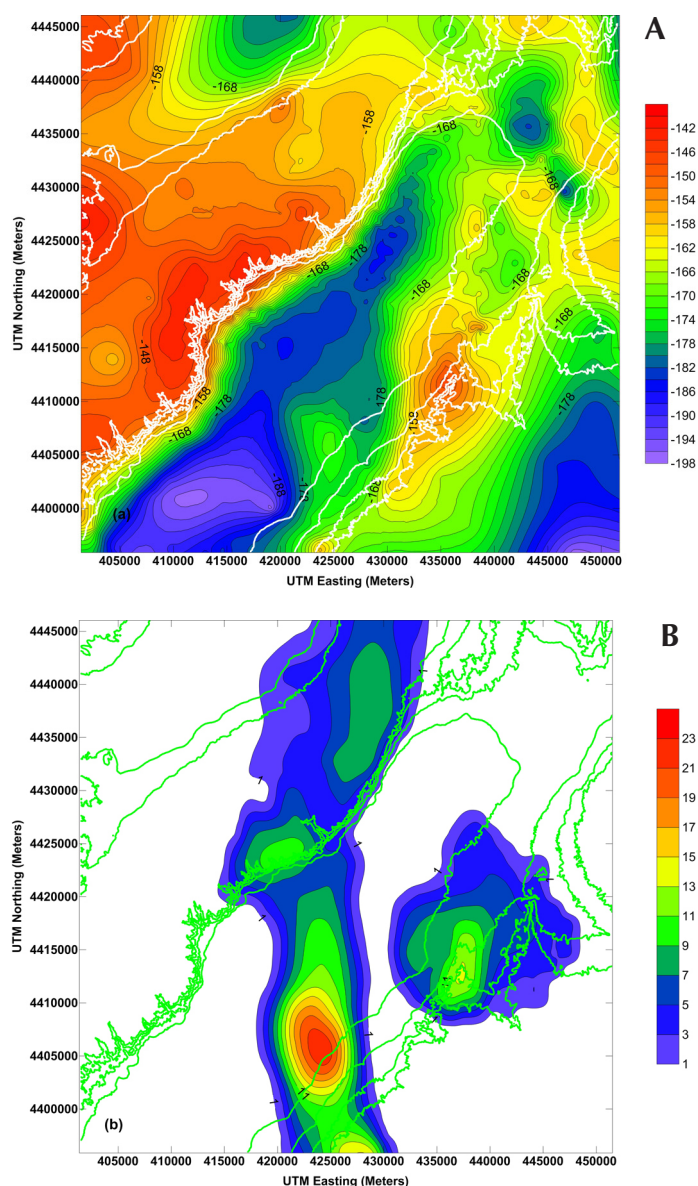


Figure 3. (a) Bouguer gravity (mgal) map of Dixie Valley EGS study area from the four gravity surveys described. (b) Pseudo gravity anomaly (mgal) used to extract the possible effect of lololith in the Dixie Valley EGS study area.

data consist of scattered lines across the valley and bench marks points; which were used to produce the Gravity Map of Nevada (Saltus, 1988). Blackwell et al. (1997) used this data set for control in producing the regional Bouguer gravity contour map. The absolute reference of this survey was an average of the gravity values available for bench marks in the area that were measured and for which gravity data are available from the US Coast and Geodetic Survey (Blackwell et al., 1997).

Merging the different gravity data sets from AMOCO (464 gravity stations), SMU data (1996 and 2000, a total 480 gravity stations), regional data (1167 gravity stations, Hittelman et al., 1994), and Pirouette Mountains (321 gravity stations, Smith, 1979) yields a total of 2432 gravity data points with complete Bouguer gravity anomaly around the Dixie valley geothermal system. Figure 3(a) shows the complete Bouguer gravity anomaly map of the study area.

Methodology: Pseudogravity

Constant magnetization of material can be converted to gravity like acceleration using the Poisson relationship, called as pseudogravity (Baranov, 1957). The relationship between the gravitational and magnetic potential caused by a body of uniform distribution of density and magnetization can be used to achieve more information of the subsurface geological structures. Pseudogravity anomalies from magnetic surveys can be used to enhance the geologic interpretation of subsurface structures, such as their depth determination. In the Stillwater Range/Dixie Valley area, Triassic marine sediments (carbonaceous shale's and siltstones, and silty limestones) of Star Peak Group are the oldest rocks (Speed, 1976). Jurassic mafic igneous complex are tectonically interleaved with the Triassic sections (Willden and Speed, 1974). The igneous rocks were originally interpreted to be an intrusive "lopolithic" body of gabbro intruded into the Jurassic and Triassic sediments (Willden and Speed, 1974; Speed, 1976). The origin of these rocks in an oceanic setting is still controversial as discussed by Dilek and Moore (1995). This unit will be referred to in this paper as the Jurassic mafic igneous complex. Magnetic data from Dixie Valley are used to model the geometry of the Jurassic mafic igneous complex (Humboldt lopolith) in the central and northern part of the study area.

The empirical relationship between mass-density and magnetic susceptibility, as compiled from Telford et al. (1990) is logarithmically-scaled, therefore is not linear (Jekeli et al., 2010, Fig 1, in the paper). This implies that main field is quite uniform in local regions; the magnetization and the mass density, in fact are not linearly related. The mass density variation may be small in the material within a volume, but the magnetic susceptibility may vary by orders of magnitude. For pseudogravity transformation of magnetic field data a susceptibility value of $S=0.2$ and density of 2.7 Kg m^{-3} was assumed, the result is shown in Fig 3b. A susceptibility value of $S=0.2$ was used to produce a pseudogravity map, that predicts a gravity anomaly of $\sim 20 \text{ mgals}$ for the Humboldt lopolith. The pseudogravity anomaly as shown in (Fig 3b) is subtracted from complete Bouguer gravity anomaly (Fig 3a) with the aim to remove a model of the effect of the lopolith from the central and northern part of the study area. The complete Bouguer gravity anomaly with modeled effect of the lopolith is shown in

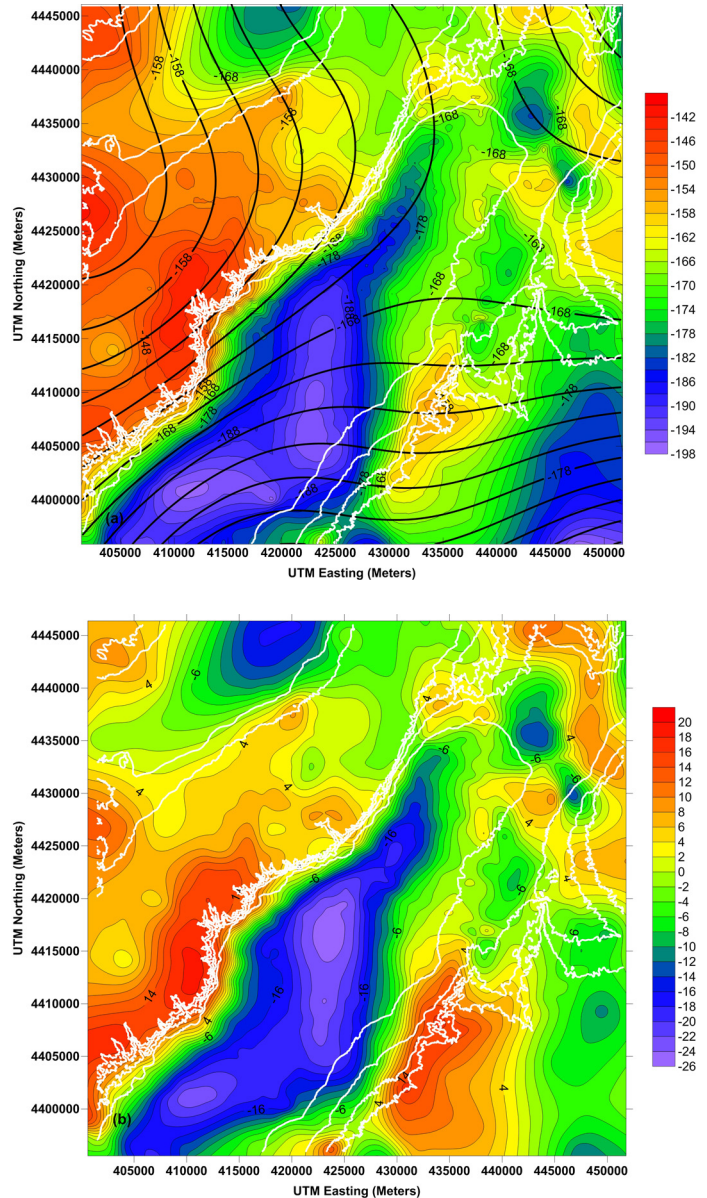


Figure 4. (a) Bouguer anomaly gravity map of Dixie Valley EGS study area after removal of Pseudo gravity anomaly. The effect of lopolith in the southern part of the valley is removed using Pseudogravity. The regional gravity contours are also shown which are used to extract residual gravity. (b) Residual gravity (mgal) of the Dixie Valley EGS study area.

Fig 4a. The basement depth inferred from gravity inversion was $\sim 400 \text{ m}$ in the southern part of Dixie Valley. The basement depth in the southern part of Dixie Valley increased by 1200 m due to lopolith removal, therefore a total basement depth in southern part is close 1600 m . The pseudogravity anomaly removed is a model and needs conformation from seismic studies of Dixie Valley which could provide more robust constrains on the location and thickness of the Humboldt lopolith.

Residual Gravity

From the complete Bouguer gravity map, which shows typical values of -190 mgal in the valley and -150 mgal in the ranges

(Figure 3a), regional gravity has been subtracted to obtain residual gravity map. Residual gravity map shown in Figure 4b, has a residual gravity variation from -26 mgal to 20 mgal. Residual gravity in the valley is -26 mgal and in the ranges is 20 mgal. The residual gravity map of Dixie Valley (Figure 4b) is used to obtain basement depth in the valley.

Inversion of Gravity Anomaly

Residual gravity data from and around Dixie Valley was iteratively inverted for basin depth using the prism method described by Cordell et al., (1968). A grid spacing of 1 km and density difference of 165 kgm⁻³ were assumed. The maximum depth inferred by the gravity inversion is 2400 m. The three dimensional basement depth map was then combined with elevation data to obtain a 3D map of the top of the basement in the area (Figure 5).

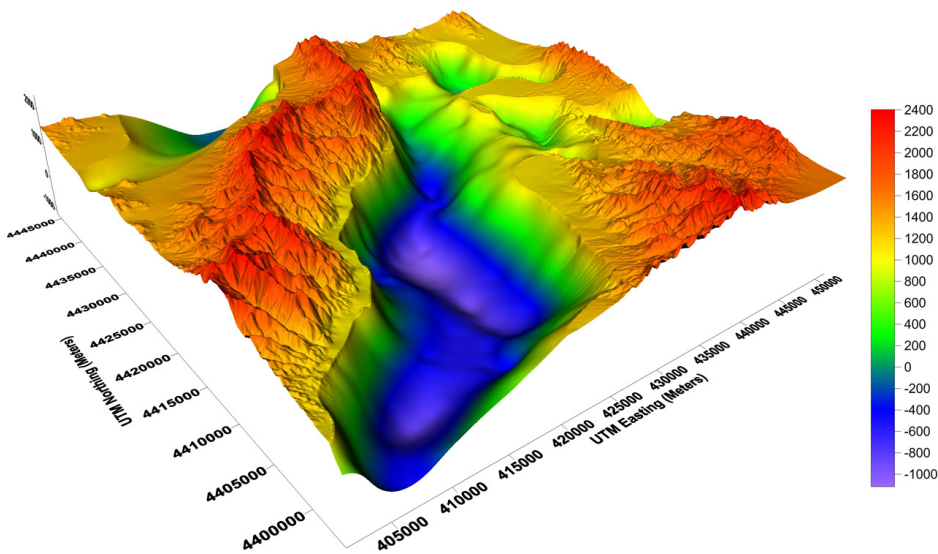


Figure 5. Three dimensional basement depth of Dixie Valley geothermal system as inferred by inversion of gravity data. Also shown is the elevation of the ranges. All heights and depths are in meters and relative to the sea level.

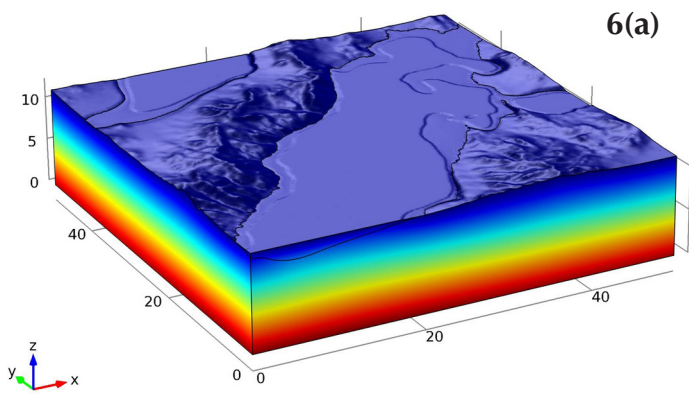


Figure 6. (a) Three dimensional conductive model of Dixie Valley. Temperatures are shown in Degree Celsius. X-axis is 50 km, y-axis is 50 km and z axis is 12 km in this model. (b) Comparison of temperature-depth curve of well 62-21 with the calculated temperature-depth curve obtained from the three dimensional model described herein.

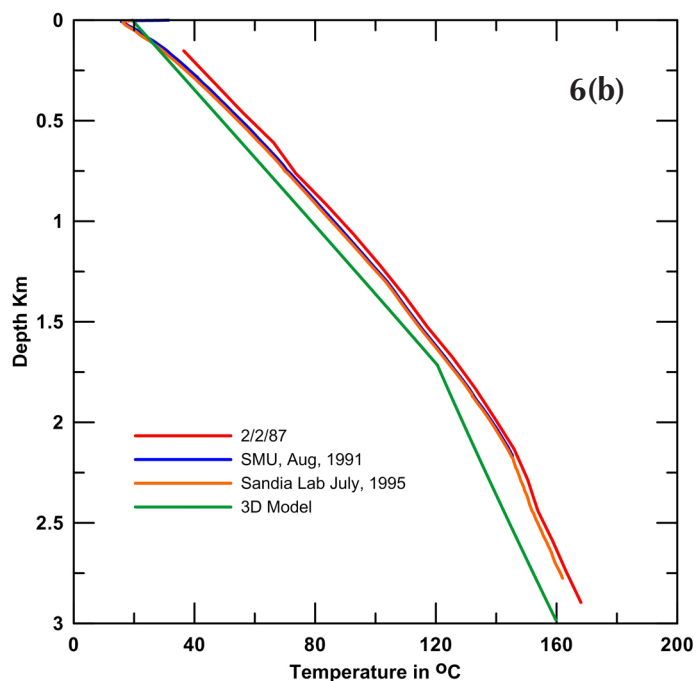
Heat Flow and Geothermal Gradient Maps of Dixie Valley

Forward modeling was used to calculate steady state subsurface temperatures of Dixie Valley project area using the model dimensions 50 km x 50 km x 12 km (Figure 6a). COMSOL multi physics software was used to generate the 3D thermal model of Dixie Valley. A thermal conductivity of 2.5 Wm⁻¹K⁻¹ is used for PreCenozoic basement and 1.25 Wm⁻¹K⁻¹ for Cenozoic valley fill sediments. The average thermal conductivity of 1.25 Wm⁻¹K⁻¹ assumed in the numerical modeling for the valley fill is lower because the sediments in the basin are probably much more clay rich on average than samples from the alluvial fans near the range front (on which thermal conductivity is measured). However, the thermal results shown by the 3D steady state conductive model are independent of effects of Humboldt lopolith in the valley.

Boundary conditions used for the model are an inward heat flux of 90 mWm⁻², a surface temperature gradient of -4 °C/Km applied to account for changes in surface temperature due to elevation from a valley surface temperature of 20 °C, and insulate sides of the model. Heat capacity at constant pressure of 1000 JKg⁻¹K⁻¹ and density of 2700 kgm⁻³ are used.

Topographic effects due to the elevation difference of ~ 1400 m between ranges and valleys control the subsurface temperatures at shallow depths. Refraction of heat flow due to the thermal conductivity contrast of a factor of 2 between valley fill sediments and basement rock also causes variation in subsurface temperatures in the model volume.

Well 62-21 (location shown in Figure 1) was used to compare the subsurface tempera-



tures of the 3D conductive model of Dixie Valley to observations. Well 62-21 represents the conductive regime of Dixie Valley, with temperature of 168°C at 2.8 km. This well is away from the thermal anomalies caused by hot fluids found along the Dixie Valley fault zone. It has been logged for temperature 3 times: in 2/2/1987, and August, 1991 by SMU Geothermal Lab and by Sandia National Lab in July, 1995 (unpublished SMU data and Williams et al., 1997). The temperature depth curves of well 62-21 and the temperature depth curve from the three dimensional conductive model are in good agreement with temperature difference less than 10 °C between the two (Figure 6b). The match would be even closer if the location of the well was only slightly moved to the west relative to the eastern edge of the antithetic fault zone.

2D Refraction of Heat Flow in Dixie Valley

Heat flows preferentially through regions of higher thermal conductivity from the interior of the Earth to the surface. In Dixie Valley, high-conductivity basement rocks are buried beneath a blanket of low conductivity sediments; heat is refracted away from the regions of thick sediment cover and preferentially channeled through thinly covered areas.

In an ideal case, where the sediment with low thermal conductivity can be considered as semicircle inside a high thermal conductivity basement rock, the heat flow with depth should be constant within the sediment basin. To study the effect of vertical variation of heat flow due to refraction, the 2D seismic cross-section Line 6 shown in Figure 1 as the red points, was modeled. The thermal results are shown along a 50 km section profile A-A' (Figure 1), where the lithology and depth of the basement is constrained by the seismic Line 6 (Figures 7a and 7b). The model dimensions are 50 km x 14 km, heat flow of 90 mWm⁻² on the bottom boundary, side walls are thermally insulated, and the top boundary is a constant surface temperature of 20 °C (Figure 7a). Basement rocks have a thermal conductivity of 2.5 Wm⁻¹K⁻¹, valley fill sediments are 1.25 Wm⁻¹K⁻¹ and basalt layer is 1.76 Wm⁻¹K⁻¹. The vertical heat flow variations due to heat refraction are shown in Figure 7c. Even though the basal heat flow is 90 mWm⁻², the calculated heat flow varies from 60-120 mWm⁻² within and around the valley

Vertical Variation of Heat Flow

To understand vertical variation of heat flow in sedimentary valley fill due to heat refraction, three vertical slices of heat flow with depth are taken at the three synthetic wells locations TD1, (17 km), TD2, (22 km) and TD3, (27.5 km) shown in Figure 1 and Figure 7c. The horizontal distances for these three hypothetical well locations shown as back squares on Figure 1, are measured from point A (0 km) of the section A-A'. The location of site TD1 is also shown in Figure 7c. Heat flow in this site decreases (Figure 7d) from 120 mWm⁻² at the surface to 90 mWm⁻² at a depth of 5 km. This site is located in basement block but it is close to the edge of the sedimentary basin. Due to the proximity of site TD1 to a large thermal conductivity contrast (the steeply dipping contact between basement rock (2.5 Wm⁻¹K⁻¹), and the sedimentary fill (1.25 Wm⁻¹K⁻¹), the high heat flow (120 mWm⁻²) is caused by

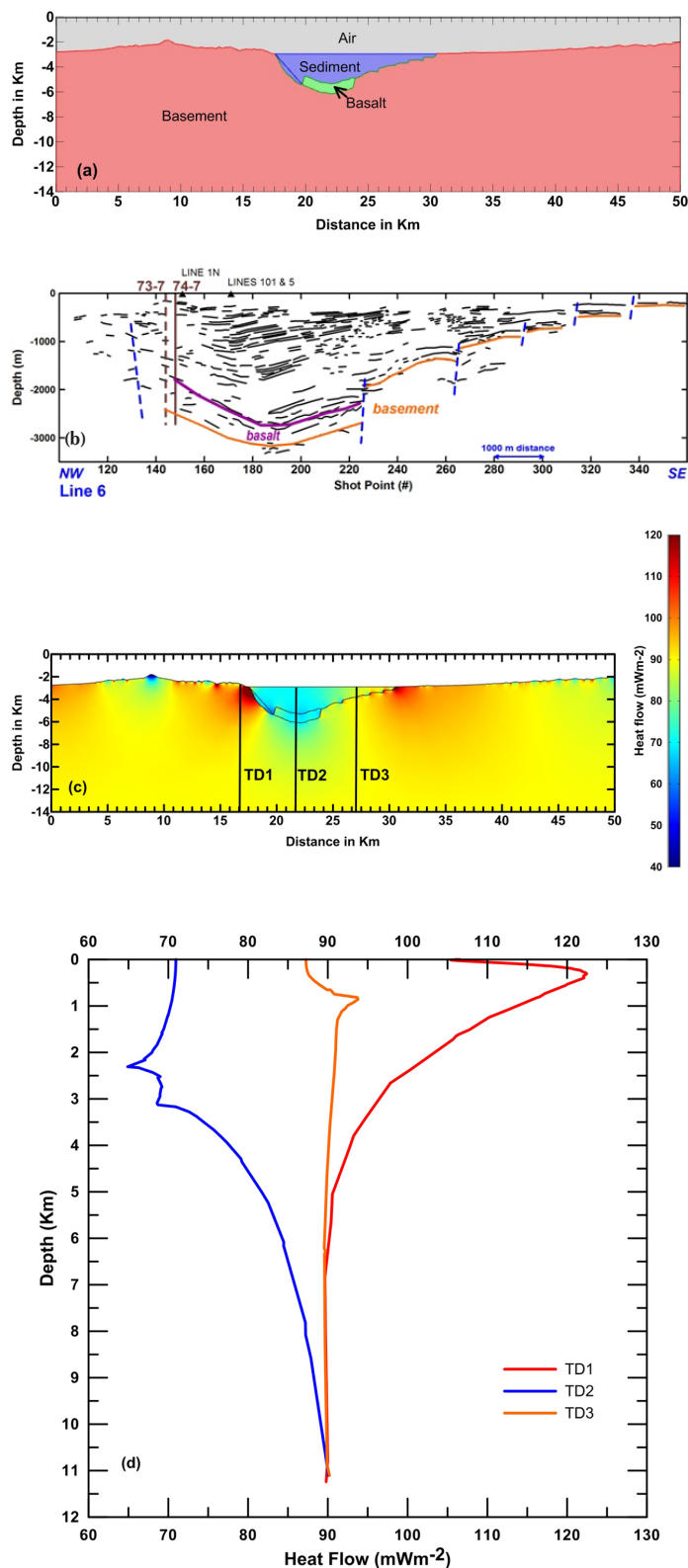


Figure 7. (a) Lithology (three rock types considered) variation along section A-A'. (b) Interpreted line drawings of the reflection section dip line 6. The vertical brown lines are wells. The blue dashed lines represents approximate fault locations, solid purple and orange are top of basalt and basement. (c) Map of heat flow variation, due thermal refraction. Synthetic wells TD1 through TD3 locations are shown in Figure 1 and Figure 7c. (d) Vertical variation of heat flow with depth for sites TD1, TD2 and TD3.

focusing of heat along the contact between basement rock and sedimentary basin (Figure 7d). Any well which is drilled in close proximity of the basin edge, will show a decrease in heat flow with depth which will be function of basin thermal conductivity contrast and shape of the contact with the basement rock accentuated by the topographic effect.

Site TD2 is located inside the sedimentary basin and intersects three lithologic layers; sediments of thickness 2-2.5 km, a basaltic layer of thickness 300-500 m, and basement rock as shown in Figure 7 (a,b,c). At site TD2 the heat flow at the surface is 72 mWm^{-2} and does not vary significantly in the sedimentary section in the depth range of 2.5 km (Figure 7d). In the basaltic layer the heat flow increases from 65 to 72 mWm^{-2} . But in the basement rock at 3 km the heat flow increases with depth from 70 mWm^{-2} to 90 mWm^{-2} at 10 km depth. In Figure 8 the heat flow contours for site TD2 show the same pattern; heat flow is constant in the sedimentary basin, but increases with depth in the basement rock. Therefore heat flow varies because of repeated thermal conductivity contrast and shape of the basin.

Site TD3 is located on the gently dipping slope on eastern edge of the Dixie Valley asymmetric basin, which has small antithetic faults (Figure 7b). Heat flow gradually increases near the surface (Figure 7c) from 60 mWm^{-2} to 90 mWm^{-2} to 120 mWm^{-2} on the western edge of the basin. Heat flow does not vary much with depth in this well, in the upper 1 km heat flow increases from 87 mWm^{-2} to 93 mWm^{-2} , there is a spike in heat flow at $\sim 1 \text{ km}$ and is due to small fault structures. Along the small faults, which are near vertical, there is a large thermal conductivity contrast of $1.25 \text{ Wm}^{-1}\text{K}^{-1}$ between sedimentary rocks and basement rocks. Due to this contrast small heat flow anomalies occur along the contact and heat flow values are discontinuous across the fault structure. These small heat flow anomalies are the spike in heat flow with depth as shown at site TD3. Below a depth of 1 km heat flow is constant at 90 mWm^{-2} .

Heat Refraction in 3D

In the specific case of Dixie Valley, a numerical solution of heat refraction must be used. The 3D conductive model shows that due to shape of the basement and the thermal conductivity contrast of 100% between sediments and the basement, the surface heat flow varies from 60-120 mWm^{-2} . The 3D conductive models also show that heat flow will not be constant with depth in the valley. Slices of heat flow at depths of 500 m below the valley floor (500 m with respect to (wrt) sea level) and 1 km below the valley floor (0 m wrt sea level), shown in Figure 8. The maximum difference in heat flow occurs close to the surface and difference in the heat flow decreases with depth. The amount of extra heat flow in ranges can be as large as 11% of the background heat flow and 25% of the heat flow observed in valleys. The percentage of difference is a function of the valley/range geometry and the magnitude of the valley/range thermal conductivity contrast.

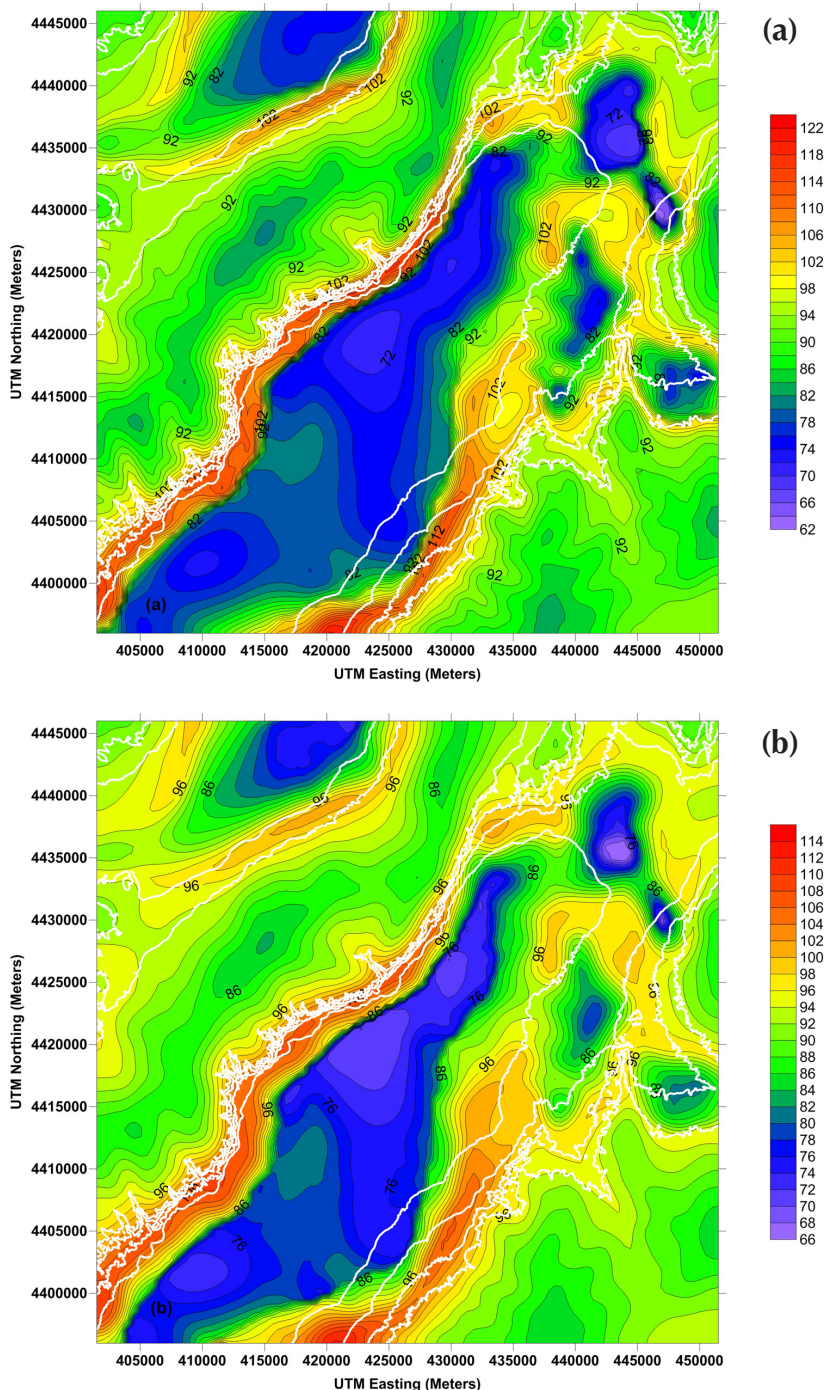


Figure 8. Heat flow slice at depth of 500 m (a) and 0 m (b) above sea level in the Dixie Valley EGS study area. Due to thermal refraction, heat flow varies from 60- 120 mWm^{-2} ; see text for details.

In Dixie Valley, heat flow in the ranges appears to be 25 % more than heat flow in the valley as shown in Figure 8.

The analysis of heat flow with depth shows that in sedimentary basins such as Dixie Valley with depth of sedimentary fill $\sim 3 \text{ km}$ and width $\sim 15\text{-}20 \text{ km}$, surrounded by basement rocks of high thermal conductivity, there are large heat refraction effects. Based on the 3D and 2D thermal models, the heat flow varies by 100% ($\sim 90 \pm 30 \text{ mWm}^{-2}$) due to the shape of the basement and the thermal conductivity contrast. Wells drilled in the vicinity (\sim

2- 5 km) of sedimentary basins edges, even in the absence of a geothermal anomaly will in general show variations in heat flow with depth. This behavior happens due to the fact that heat flow is focused along the edges of the basins; in other words more heat is flowing than the background in the basement rocks near the edge of the basin. Because of this, wells drilled in the basement rock near the edge of sedimentary basins will show a decrease in heat flow with depth; i.e. changes in gradient with depth will not be accounted by thermal conductivity variation in the well.

3D Conductive Subsurface Temperatures in Dixie Valley

The thermal regime in the BRP is complicated because of the complex structure and geologic history. The complexity involves both conductive and convective thermal effects. In Dixie Valley major conductive complexities are due to (1) the difference in

thermal properties in the valleys, (2) the ranges and the resulting refraction effects between the valleys and the ranges, and (3) effects of the topography on the thermal regime. The convective effects are related to large scale deep circulation of meteoric fluids related to the generation of the BRP geothermal systems and to shallow hydrologic effects due to the topography and the geology. Hence the thermal regime can be quantified only if extensive thermal data are available. So development of an independent prediction of temperature would be a step forward in the regional and local geothermal resource delineation in the Great Basin. The basis of the analysis of the thermal regime for the BRP in general and Dixie Valley particularly is described.

A full 3D steady state temperature of the study area is shown in Figure 6a. Slices of temperature at various depths relative to the sea level were produced at 1000 m, 0 m, -1000 m, -2000 m, -3000 m and -4000 m (Figure 9). These temperature depth maps take into account the elevation difference between ranges and valley and the thermal conductivity difference between valley fill sediments and the country rocks. They are based on the assumption of a conductive heat transfer averaging 90 mWm^{-2} and an average thermal conductivity ratio of 1:2 between sediment fill and basement. These temperatures represent a base state for comparison of the thermal effects of convection and as a base case for the effects of temperature in other geophysical property models.

At 1000 m asl elevation, close to the mean elevation of Dixie Valley (1100 m asl), temperatures are higher in the ranges compared to the valley (Figure 9). At a depth of 1 km beneath the valley floor the conductive steady state temperatures are higher in the valley (0 m asl level slice, Figure 9 a) compared to the ranges. Below 1 km depth, the valley always has higher temperatures than the ranges. At a depth of 4 km (-4000 m below the valley floor) the maximum conductive steady state temperature reaches a predicted value of 248°C (Figure 9). Therefore, the 3-D temperature model improves the resolution of crustal geothermal structure estimates in the Dixie valley for EGS geothermal resources and can be used to compare the temperature estimate from other geophysical techniques in the Dixie Valley.

Due to lopolith removal the sediment thickness increased from 400 m to 1600 m in the southern part of the Dixie Valley study area. Temperature increased from 88°C to 123°C at 1.6 km after lopolith removal, temperature increases because sediment thickness of low thermally conductivity $1.25 \text{ Wm}^{-1}\text{K}^{-1}$ increased by 1200m. The lopolith temperature effect decreases with depth, e.g., at a depth of 5km temperatures are 230°C , which are 22°C hotter because of lopolith removal.

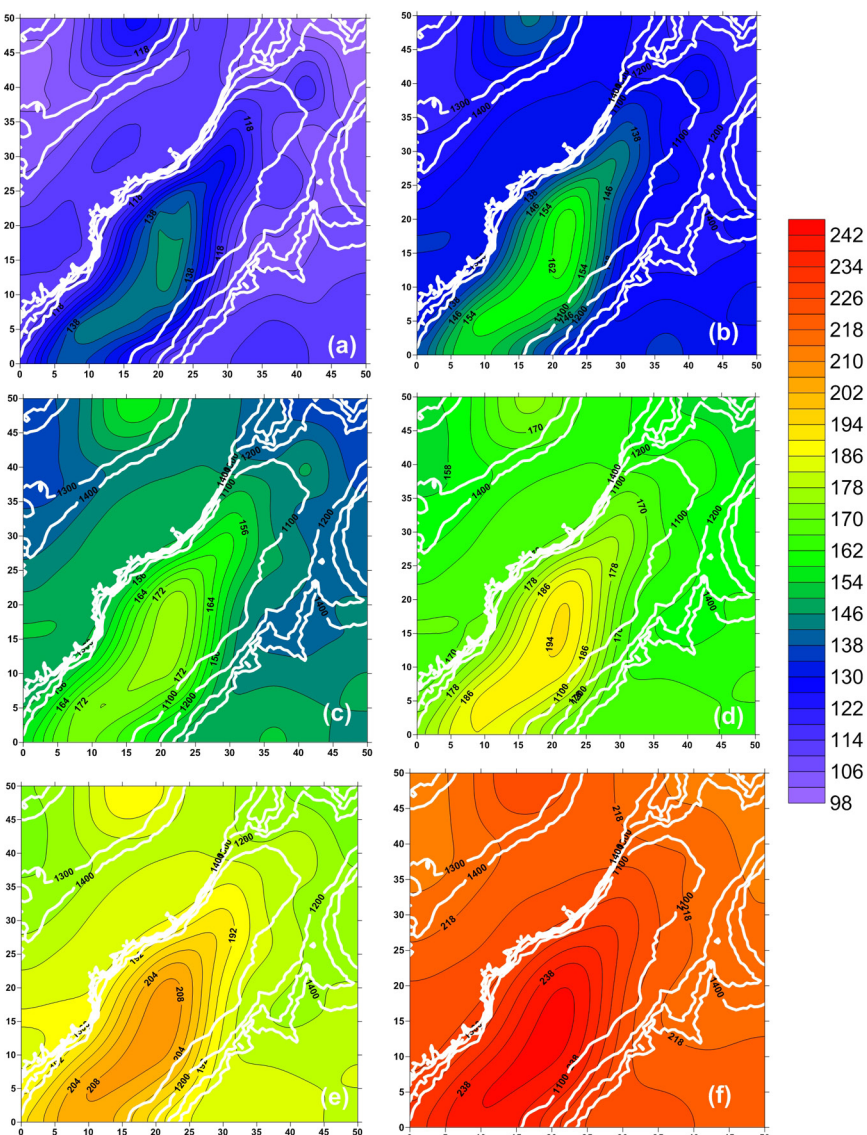


Figure 9. Temperature slices of the EGS study area at various depths relative to the sea level, (a) -1000 m, (b) -1500 m, (c) -2000 m, (d) -2500 m, (e) -3000 m, (f) -3500 m and (g) -4000 m. Temperatures are in degree C.

Conclusions

The Humboldt lopolith in the central and northern part of the Dixie Valley will cause high velocities in the seismic studies causing difficulty

in the interpretation of the basement depth. Therefore lopolith removal using magnetic data increases sediment thickness in the central and northern part of Dixie Valley is open to various interpretations and needs to be confirmed after a seismic study of the central and northern part of the Dixie Valley. Temperature increases by 33 oC at 1.6 km and 22 oC at 5 km due to lopolith removal have been modeled. A maximum of 248 oC temperature is reached at a target depth of 5 km in the Dixie Valley using a three dimensional conductive steady state model. Comparisons of temperature-depth curves from well 62-21 with 3D conductive thermal models predict less than 10 oC temperature difference at depth of ~3 km. Heat flow variation with depth in a well will depend on well location in/around the sedimentary basin and the magnitude of thermal conductivity contrast between sediments and the basement rocks. Due to topographic effects and heat refraction isotherms will be compressed in the Dixie Valley. The heat flow in the ranges is higher compared to the valley for same elevation and the difference between heat flow in these two environments decreases with depth. This study can be applied to estimate regional heat flow in Basin and Range Province.

Acknowledgments

The data presented in this study were collected by the authors and several other individuals. This study has been supported by DOE contract no. DE-EE0002778 to AltaRock Energy Inc.

References

- Baranov, V., 1957. A new method for interpretation of aeromagnetic maps-pseudogravity anomalies. *Geophysics*, v. 22, p. 359-383.
- Bell, J.W., and T. Katzner, 1987. Surficial geology, hydrology and late Quaternary tectonics of the IXL Canyon area, Nevada; Nevada Bureau of Mines and Geology Bulletins, v. 102, p. 1-52.
- Blackwell, D.D., B. Gollan, and D. Benoit, 2000. Temperatures in the Dixie Valley, Nevada geothermal system. *Geothermal Resources Council Transactions*, v. 24, p. 223-228.
- Blackwell, D.D., A. Waibel, and S.A. Kelly, 1994. Results of Dixie Valley Power Partners/Oxbow 1994 thermal gradient drilling program, Report.
- Blackwell, D.D., R.S. Smith, and M.C. Richards, 2007. Exploration and development at Dixie Valley Nevada; Summary of DOE studies, Proceedings 32th Workshop on Geothermal Reservoir Engineering, Stanford Geothermal Program Report SGP-TR-183.
- Blackwell, D.D., K. Wisian, D. Benoit, and B. Gollan, 1999. Structure of the Dixie Valley geothermal system, a "typical" Basin and Range geothermal system, from thermal and gravity data. *Geothermal Resources Council Transactions*, v.23, p.525-531.
- Blackwell, D.D., 1983. Heat flow in the Northern Basin and Range Province. *Geothermal Resources Council, Special Report No. 13*, p. 81-92.
- Blackwell, D.D., J.L. Steele, and L.S. Carter, 1991. Heat-flow patterns of the North American continent: a discussion of the Geothermal Map of North America. In: Slemmons, D.B., Engdahl, E.R., Zoback, M.D., Blackwell, D.D. (Eds.), *Neotectonics of North America. Decade Map*, v. 1, Geological Society of America, Boulder, CO, p. 423-436.
- Blackwell, D.D., and K. Wisian, 1997. Gravity Analysis of Dixie Valley, Nevada Geothermal System; Report submitted to Oxbow Geothermal Corporation, Reno, Nevada.
- Cordell, L., and R.G.Henderson, 1968. Iterative three-dimensional solution of gravity anomaly data using a digital computer. *Geophysics*, v.33, p.596-601.
- Dilek, Y., and M.M. Eldridge, 1995. Geology of the Humboldt igneous complex, Nevada, and Tectonic implications for the Jurassic magmatism in the Cordilleran Orogen. *GSA Special*, v. 290, p. 229-248.
- Grauch, V.J.S., 2002. High-resolution Aeromagnetic Survey to Image Shallow Faults, Dixie Valley Geothermal Field, Nevada. U.S. Geological Survey Open-File Report, 02-384.
- Hittelman, A. M., D.T. Dater, R.W. Buhmann, and S.D. Racey, 1994. Gravity-1994 edition CD-ROM user's manual, NOAA Natl. Geophys. Data Center, Boulder, Colo.
- Iovenitti J.L., D. D. Blackwell, J.S.Sainsbury, I.M. Tibuleac, A.F.Waibel, T.T. Cladouhos, R.Karlin, B.M. Kennedy, E. Isaaks, P.E.Wannamaker, M.T. Clyne, O.C.Callahan, 2011. "EGS Exploration Methodology Development Using the Dixie Valley Geothermal District as a Calibration Site, A Progress Report," *Geothermal Resources Council Transactions*, v. 35, p. 12.
- Jekeli, C., K.Erkan, O. Huang, 2010. Gravity vs pseudogravity: A comparison based on magnetic and gravity gradient measurements. *Earth and Environmental Science*, v. 135, Part 1, 123-127,
- Kennedy, B.M., T.P.Fischer, and D.L. Shuster, 2000. Heat and helium in geothermal systems, Proceedings 25th Workshop on Geothermal Reservoir Engineering, Stanford Geothermal Program Report SGP-TR-165, p. 167-173.
- Kucks, R.P., P.L. Hill, D.A. Ponce, and D.A., 2006. Nevada magnetic and gravity maps and data: A website for distribution of data by USGS. URL:<http://pubs.usgs.gov/ds/2006/234/data/>.
- Lachenbruch, A.H., and J.H. Sass, 1977. Heat flow in the United States and the thermal regime of the crust. In: Heacock, J.G. (Ed.), *The Nature and Physical Properties of the Earth's Crust*. American Geophysical Union Monograph, v. 20, p.626-675.
- McKenna, J.R., and D.D.Blackwell, 2004. Numerical modeling of transient Basin and Range extensional geothermal Systems. *Geothermics*, v. 33, p. 457-476.
- Saltus, R. W., 1988. Regional, residual and derivative gravity maps of Nevada; Nev. Bur. Mines and Geol. Map 94B, 1:1,000,000.
- Smith, R.D., 1979. Geophysical Report: Magnetotellurics, gravity, magnetics in Dixie Valley Nevada. Geotronics Corp., Austin, TX, p.53, plus 7 Plates.
- Speed, R.C., 1976. Geologic map of the Humboldt Lopolith. Geological Society of America Map and Chart Series MC-14, 1:81050 Scale, 4p.
- Telford, W.M., L.P. Geldart, and R.E. Sheriff, 1990. *Applied Geophysics*, 2nd ed. Cambridge U. Press, Cambridge, U.K.
- Williams, C.F., J. H. Sass, and F.V. Grubb, 1997. Thermal signature of subsurface fluid flow near the Dixie Valley geothermal Filed Nevada., Proceedings 22th Workshop on Geothermal Reservoir Engineering, Stanford Geothermal Program Report SGP-TR-155, 161-168.
- Willden, R. and R. C. Speed, 1974. Geology and mineral deposit of Churchill County, Nevada. Nevada Bureau of Mines and Geology Bulletin 83, 95p, 1:250,000.
- Wright, P.M., 1991. Exploration for new hydrothermal resources for electrical power generation in the 48 contiguous U.S. states. *Geothermal Resources Council Transactions*, v.15, p. 217-228.

